

Original Article

# Gene expression analysis of antioxidant and DNA methylation on the rat liver after 4-week wood preservative chromated copper arsenate exposure

Naofumi Takahashi<sup>1\*</sup>, Satoru Yamaguchi<sup>1</sup>, Ryouichi Ohtsuka<sup>1</sup>, Makio Takeda<sup>1</sup>, Toshinori Yoshida<sup>2</sup>, Tadashi Kosaka<sup>1</sup>, and Takanori Harada<sup>1</sup>

<sup>1</sup> The Institute of Environmental Toxicology, 4321 Uchimoriya-machi, Joso-shi, Ibaraki 303-0043, Japan

<sup>2</sup> Laboratory of Veterinary Pathology, Tokyo University of Agriculture and Technology, 3-5-8 Saiwai-cho, Fuchu-shi, Tokyo 183-8509, Japan

**Abstract:** Our previous 4-week repeated dose toxicity study showed that wood preservative chromated copper arsenate (CCA) induced hepatocellular hypertrophy accompanied by biochemical hepatic dysfunction and an increase in oxidative stress marker, 8-hydroxy-deoxyguanosine, in female rats. To further explore the molecular mechanisms of CCA hepatotoxicity, we analyzed 10%-buffered formalin-fixed liver samples from female rats for cell proliferation, apoptosis, and protein glutathionylation and conducted microarray analysis on frozen liver samples from female rats treated with 0 or 80 mg/kg/day of CCA. Chemical analysis revealed that dimethylated arsenical was the major metabolite in liver tissues of male and female rats. CCA increase labeling indices of proliferating cell nuclear antigen and decrease terminal deoxynucleotidyl transferase-mediated dUTP nick-end labeling accompanied with increased expression of protein glutathionylation, indicating a decrease in glutathione (GSH) in hepatocytes of female rats. Microarray analysis revealed that CCA altered gene expression of antioxidants, glutathione-S-transferase (GST), heat shock proteins and ubiquitin-proteasome pathway, cell proliferation, apoptosis, DNA methylation, cytochrome P450, and glucose and lipid metabolism in female rats. Increased expression of GSTs, including *Gsta2*, *Gsta3*, *Mgst1*, and *Cdkn1b* (*p27*), and decreased expression of the antioxidant *Mt1*, and DNA methylation *Dnmt1*, *Dnmt3a*, and *Ctcf* were confirmed in the liver of female rats in a dose-dependent manner. Methylation status of the promoter region of the *Mt1* was not evidently changed between control and treatment groups. The results suggested that CCA decreased GSH and altered the expression of several genes, including antioxidants, GST, and DNA methylation, followed by impaired cell proliferation in the liver of female rats. (DOI: 10.1293/tox.2022-0093; J Toxicol Pathol 2023; 36: 31–43)

**Key words:** chromated copper arsenate, DNA methylation, glutathione, liver, metallothionein, oxidative stress

## Introduction

The wood preservative chromated copper arsenate (CCA) has long been used to protect wood products from pests and fungi for outdoor use<sup>1</sup>. However, due to human health concerns regarding arsenic-containing CCA, the US Environmental Protection Agency announced in 2003 that CCA manufacturers had voluntarily ceased manufacturing CCA pressure-treated household wood and opted to provide consumers with wood products treated with an alternate wood preservative<sup>2, 3</sup>. Many other countries have also limited the use of CCA as a wood preservative<sup>4</sup>. CCA-treated

woods, however, are still used in our living environment and remain a source of environmental arsenic pollution<sup>1</sup>. The high release of arsenic was confirmed with experiments using a CCA-treated deck exposed to rainfall, and 13% of the arsenic was leached from the amount initially present in the CCA-treated wood during a 3-year-monitoring period. This indicates that exposure of the CCA-treated deck to rainfall resulted in elevated arsenic concentrations in both the runoff and soil<sup>5</sup>. When comparing the surface soil from underneath CCA-treated playground structures at 16-years after installation with that at 26-years after installation, the concentration of arsenic increased during the 10 years, and the structures might continue to be a source of elevated arsenic exposure to children<sup>6</sup>. Arsenic released from CCA-treated dimensional lumber poses a potential risk to contaminate groundwater<sup>7</sup> and to then be taken up by plants<sup>8</sup>. Lumber debris after the Great East Japan Earthquake and tsunami could be the source of arsenic and chromium in the environment and a hazard to human health<sup>9</sup>, suggesting that CCA exposure may be caused by similar global events.

The biological effects of CCA are complicated because

Received: 30 August 2022, Accepted: 16 September 2022

Published online in J-STAGE: 9 October 2022

\*Corresponding author: N Takahashi (e-mail: n.takahashi@iet.or.jp)

©2023 The Japanese Society of Toxicologic Pathology

This is an open-access article distributed under the terms of the Creative Commons Attribution Non-Commercial No Derivatives

(by-nc-nd) License. (CC-BY-NC-ND 4.0: <https://creativecommons.org/licenses/by-nc-nd/4.0/>).



of the presence of arsenic, chromium, and copper as constituents. These constituents are absorbed in the gastrointestinal tract and distributed in the liver, posing a risk of liver failure<sup>1, 2</sup>. While there have been numerous reports of toxicity assessments of arsenic, chromium, and copper individually, there are a limited reports of toxicity assessments of CCA, in which acute toxicity and teratogenicity of the combinations of these constituents were reported in rats<sup>10, 11</sup>. We previously reported that CCA exposure induced anemia, blood lipid and glucose alterations, and dysfunction of the gastrointestinal tracts, kidney, and liver in a 4-week oral toxicity study in rats, and this was accompanied with higher plasma levels of arsenic than chromium<sup>12</sup>. In the liver, we found that CCA caused hepatocellular hypertrophy with hypoproteinemia, hyperglycemia, hypercholesteremia, high  $\gamma$ -glutamyl transpeptidase and total bilirubin, and an increase in the oxidative stress marker, 8-hydroxydeoxyguanosine (8-OHdG) in female rats<sup>12</sup>; however, the mechanism of hepatotoxicity of CCA remains uncertain. The liver is the major organ for arsenic methylation metabolism<sup>13, 14</sup> and may be a potential target for arsenic-induced cancer<sup>15</sup>. Exposure to arsenic can cause oxidative stress in the liver by reducing anti-oxidative enzymes<sup>16</sup>. In this study, to elucidate possible mechanism of hepatotoxicity in female rats treated with CCA, we examined the impaired balance between cell proliferation and apoptosis in hepatocytes that might be accompanied with accumulation of arsenic species, altered gene expression of antioxidants, and DNA methylation determined by combined microarray and quantitative RT-PCR of liver samples.

## Materials and Methods

### *Chemicals and route of exposure*

Among the CCA types A, B, and C, we prepared a CCA type B mixture containing arsenic (V) oxide (45.1% as As<sub>2</sub>O<sub>5</sub>, w/w), chromium (VI) oxide (35.3% as CrO<sub>3</sub>, w/w), and copper (II) oxide (19.6% as CuO, w/w)<sup>17</sup>. Arsenic oxide was purchased from Kishida Chemical Co., Ltd. (Osaka, Japan) and chromium oxide and copper oxide from Kanto Chemical Co., Inc. (Tokyo, Japan). Arsenic oxide and chromium oxide were dissolved in saline, and copper oxide was suspended in the mixture. Ten Wistar Hannover specific pathogen-free (SPF) (BrlHan:WIST@Jcl[GALAS]) rats (Japan Clea, Inc., Shizuoka, Japan) per sex per group received daily gavage administration of CCA at dose levels of 0, 8, 40, and 80 mg/kg/day for 28 days as described previously<sup>12</sup>. During the study, all animals were handled in accordance with the Guidelines for Animal Experimentation issued by the Japanese Association for Laboratory Animal Science<sup>18</sup> and with the Code of Ethics for Animal Experimentation of the Institute of Environmental Toxicology.

### *Tissue samples*

The median lobes of the liver from female rats treated with a dose level of 0 or 80 mg/kg/day were fixed in 10% buffered formalin solution, sectioned, and stained with hematoxylin and eosin (H&E) for histopathological examina-

tion. The paraffin sections were used for immunohistochemistry and terminal deoxynucleotidyl transferase-mediated dUTP nick-end labeling (TUNEL) in this study. The other frozen liver lobe samples obtained from female and/or male rats treated with 0, 8, 40, or 80 mg/kg/day of CCA were used for analysis of arsenicals, microarray, quantitative RT-PCR, and DNA methylation analyses.

### *Chemical analysis of arsenicals in the liver*

Liver samples from three male and female rats treated with 80 mg/kg/day of CCA were stored at  $-70^{\circ}\text{C}$ , and five arsenical species, including arsenate (As[V]), arsenite (As[III]), and methylated forms, i.e., monomethylated-arsenic (MMA), dimethylated-arsenic (DMA), and trimethylated-arsenic (TMA), were measured by high-performance liquid chromatography (Agilent 1200 series, Agilent Technologies, Santa Clara, CA, USA) and inductively coupled plasma mass spectrometry (Agilent 7500ce ICP-MS, Agilent Technologies).

### *Immunohistochemistry, TUNEL, and analysis of immunopositive reactions*

Immunohistochemistry was performed as previously reported<sup>19</sup>. Paraffin sections obtained from the livers of six female rats in order of ascending animal numbers each in the CCA 0 and 80 mg/kg/day groups were incubated with monoclonal antibodies against proliferating cell nuclear antigen (PCNA) ( $\times 1,000$ ; Dako, Glostrup, Denmark) and glutathione (GSH) ( $\times 100$ ; Abcam, Cambridge, MA, USA). Under oxidative stress, GSH plays a prominent role in protein redox regulation via S-glutathionylation, i.e., the conjugation of GSH to reactive protein cysteine residues to protect it from oxidative damage<sup>20</sup>. We visualized S-glutathionylated proteins (PSSG) in the liver using immunohistochemistry with anti-GSH antibody. The sections were pretreated by autoclave in a citrate buffer pH 6.0 at  $121^{\circ}\text{C}$  for 5 min for antigen retrieval. The paraffin sections obtained from the same six females selected for immunohistochemistry were used for TUNEL analysis with an Apoptag peroxidase *in situ* apoptosis detection kit (Merck Millipore, Billerica, MA, USA) performed according to the protocol recommended by the manufacturer. Duodenum tissues were used as the positive control for both PCNA and TUNEL stains and positive reactions were observed from these stains. For the negative control, phosphate-buffered saline replaced the primary antibodies. To determine the PCNA or TUNEL-positive hepatocyte ratio, 1,000 hepatocytes were manually counted with a light microscope, as previously reported<sup>21</sup>. The PCNA labeling index (LI) or TUNEL index was calculated by dividing the number of labeled nuclei by the total number of nuclei counted, and the results were expressed as percentages. The ratio of PCNA and TUNEL was calculated. GSH-stained specimens were semi-quantitatively graded according to the extent of positive areas in the liver lobules (Positive area: slight,  $<10\%$ ; moderate,  $10\text{--}50\%$ ; severe,  $>50\%$ ).

### Extraction of RNA and DNA

The frozen samples were stored at  $-70^{\circ}\text{C}$  until required for analysis. Total RNA and DNA were extracted from female liver tissues using the RNeasy Mini kit (QIAGEN K.K., Tokyo, Japan) and the DNeasy Tissue Kit (QIAGEN K.K.), respectively. The concentrations of RNA and DNA were measured using a spectrophotometer (GeneQuant pro; GE Healthcare Japan, Tokyo, Japan). These nucleic acid samples were stored at  $-70^{\circ}\text{C}$  until required.

### Microarray analysis

We performed comprehensive gene expression analysis on female rat livers. Each microarray analysis was performed for the comparison between the CCA 0 and 80 mg/kg/day groups on three array slides. To adjust for scale differences among the slides, a pooled RNA control sample was prepared from CCA 0 mg/kg/day samples and used as a reference for each sample, according to a previously reported method<sup>22</sup>. Cyanine 3 (Cy3)-labeled reference probes were synthesized from pooled CCA 0 mg/kg/day RNA samples, and cyanine 5 (Cy5)-labeled sample probes were synthesized from RNA derived from the CCA 0 and 80 mg/kg/day groups by using the Fluorescent Direct Label Kit (GE Healthcare Japan) according to the protocol recommended by the manufacturer. Cy3-labeled reference probes and Cy5-labeled sample probes were combined and hybridized to a cDNA microarray slide (Intelligene, TaKaRa Bio Inc., Shiga, Japan) containing approximately 2,000 genes according to manufacturer's recommended protocol. The microarray slides were scanned with a microarray scanner (ScanArray lite; Perkin-Elmer Bioscience Japan, Tokyo, Japan). The criteria for gene expression were determined in accordance with a previously reported method<sup>22</sup>. We selected the genes that showed a greater than 2-fold change compared with that in the control group.

### Validation of microarray with quantitative RT-PCR

Microarray analysis data were validated with the quantitative RT-PCR method using the liver samples obtained from all females in the CCA 0, 8, 40, and 80 mg/kg/day groups. The following mRNAs were selected for measurement based on the microarray data: metallothionein 1 (*Mt1*), glutathione S-transferase alpha 2 (*Gsta2*), microsomal glutathione S-transferase 1 (*Mgst1*), cyclin-dependent kinase inhibitor 1B (*Cdkn1b/p27*), and CCCTC-binding factor (*Ctcf*). Expression levels of mRNA for glutathione S-transferase alpha 3 (*Gsta3*), DNA methyltransferase 1 (*Dnmt1*), and DNA methyltransferase 3 alpha (*Dnmt3a*) were additionally examined to further confirm the roles of glutathione S-transferase (GST) and DNA methylation on CCA-induced hepatotoxicity, based on the microarray data. Primer and probe sets corresponding to each gene were purchased from Nippon Gene (Toyama, Japan). Sequences of these primer sets are shown in Table 1. Glyceraldehyde-3-phosphate dehydrogenase mRNA (*Gapdh*) was used as an internal standard to normalize the expression data and the primer and probe sets were purchased from Applied Biosystems Japan

Ltd. (Tokyo, Japan). PCR standards were made from PCR products amplified using primer sets corresponding to each gene. The concentration of the total RNA extracted from the liver tissues was prepared to a concentration of 0.1  $\mu\text{g}/\mu\text{L}$ , and 0.5  $\mu\text{g}$  of prepared RNA was reverse transcribed in a 50  $\mu\text{L}$  PCR reaction using TaqMan RT reagents (Applied Biosystems Japan Ltd.). For each gene, cDNA, primer set, and AmpliTaq Gold PCR Master Mix (Applied Biosystems Japan Ltd.) were prepared to 50  $\mu\text{L}$  with ultra-purified water (Nihon Millipore K.K., Tokyo, Japan), and PCR reaction was performed in a PCR thermal cycler (TaKaRa Bio Inc.). Thereafter, PCR products were purified with QIAquick PCR Purification Kit (Qiagen K.K.) and their concentration (DNA) was measured using a spectrophotometer (GeneQuant pro). PCR products were prepared to 10 nM with ultra-purified water by the calculation of each concentration, length, and sequence, and these samples were kept at  $-70^{\circ}\text{C}$  until use. For analytical samples, the concentration of total RNA extracted from the liver tissues was prepared to 0.1  $\mu\text{g}/\mu\text{L}$ , and 0.4  $\mu\text{g}$  of the sample was reverse transcribed in a 40  $\mu\text{L}$  PCR reaction using TaqMan RT reagents. For the PCR standards, 10-fold dilutions were prepared, and five serial points were used. In the quantitative RT-PCR, cDNA of samples, dilutions of standard DNA, primer/probe set, and TaqMan Universal PCR Master Mix (Applied Biosystems Japan Ltd.) were prepared to 25  $\mu\text{L}$  with ultra-purified water using ABI PRISM 7700 (Applied Biosystems Japan Ltd.). Data are given as ratios relative to *Gapdh* expression.

### Methylated DNA immunoprecipitation PCR

To verify the DNA methylation changes in the promoter region of rat *Mt1*, methylated DNA was captured and quantified using methylated DNA immunoprecipitation (MeDIP) coupled with quantitative PCR analysis. Quantitative MeDIP-PCR was performed on liver tissues from six female rats in order of ascending animal numbers each from the CCA 0 and 80 mg/kg/day groups. Methylated DNA was isolated by means of Methylamp Methylated DNA Capture Kit (Epigentek Group Incorporation, Farmingdale, NY, USA). Briefly, 2  $\mu\text{g}$  of DNA was sheared with a Bioruptor<sup>TM</sup> (Cosmo Bio co., Ltd., Tokyo, Japan) set on high with 7 cycles of 20 s ON and 60 s OFF. An aliquot of this DNA was used for immunoprecipitation with 5-methylcytosine antibody (IP), and others were used as the input DNA (Input). DNA was prepared from the IP and Input samples using a QIAquick PCR Purification Kit. Quantitative PCR was performed as described above. CpG islands (CGI) were identified by using Methyl Primer Express (Applied Biosystems Japan Ltd.) and CpGenome with the MethPrimer (<http://www.urogene.org/methprimer/index1.html>) online service. Primer and probe sets were purchased from Bio Technologies Japan (Tokyo, Japan). The sequences of these sets and the location from the transcription start site (TSS) are shown in Table 2. Three primer and probe sets were designed to cover the DNA sequence of non-CGI site located about 1100 bp upstream of the TSS (nCGI), first CGI (CGI 1), and third CGI closest to the TSS (CGI 2) of rat *Mt1*. Methylation status

**Table 1.** Primer and Probe Sets for Quantitative Reverse Transcription Polymerase Chain Reaction (RT-PCR)

Gene symbol	Sequence			Amplicon size (bp)
	Forward primer	Reverse primer	TaqMan probe	
<i>Mtl</i>	TTCACCAGATCTCGGAATGGA	ACACAGCCCTGGGCACAT	CTCCAGCTCCTGCGGCTGCAA	124
<i>Gsta2</i>	TTTGATGAGAAGTTTATACAGAGTCCAGA	ACCATGGGCACCTTGGTCAA	TGGAAAAGCTAAAGAAGACGGGAATTTGA	86
<i>Gsta3</i>	GGACCCAGGCATTTGGGA	CAGGCTGAAGAAACTTCTTCACTGT	TTCCCTCTGCTAAAGGCCCTGAGAACC	92
<i>Mgstl</i>	AGTTCCCTTCGGACTGACGAGAA	GATACCGAGAAAGGGAACGATGT	ACGGGTGGGAAGAGCCACC	86
<i>Cdhn1b</i> (p27)	GGTCAATCATGAAGAATA	AGTCGA AATTCCACTTG	CTCGCTTCTTCCATATCTCGGCA	86
<i>Dnmt1</i>	ACCAGGCAGACCACCATCA	TGGCTTCCCTTTTCAGAGTCT	TCAC TTCAAGGGTCCCGCTAAACGG	81
<i>Dnmt3a</i>	ATAAGCTGGAGTTGCAAGAGTGTCT	CTTTATGGAGTTTGACCTGGTGTA	CGGCAGAATAGCCAAGTTCAGCAAAGTG	92
<i>Ctcf</i>	GTCCCCACTGTGACACTGTCA	ACACAGCATCACAGTAGCGACAT	AGTGATTTGGGTGTCCACTTGAGAAAGCA	111

**Table 2.** Primer and Probe Sets for Quantitative Methylated DNA Immunoprecipitation Polymerase Chain Reaction (MeDIP-PCR)

Name	Location	Sequence			Amplicon size (bp)
		Forward primer	Reverse primer	TaqMan probe	
nCGI	(-1)172 - (-)1074	GGCATAATCATCATATCGCACAGT	CATTGGTTCACGGCTACTCAGA	AGGTCCTATAACAGTTAAGC	98
CGI1	(-7)98 - (-)648	CGCTTCCCTAGGTAAGCGCTTAC	TCGCAACATATTTCCCCACTCA	TAGAGCCGATGGCTAAA	151
CGI2	(-94 - (-)11	GAGAGCAGACTGTCCGCTAAGC	GTGAATCTGGAGCAACGGTGTGA	CATCCCGACTTCAGC	84

Location indicates the position from the transcription start site.

in the promoter region of *Mtl* is presented as the ratio (%) between IP and Input.

### Statistical analysis

The following statistical methods were used to determine the significance of differences in the results between the treated and control groups ( $p \leq 0.05$  or  $0.01$ ): Dunnett's multiple comparison test for quantitative RT-PCR; and Student's *t*-test or Aspin–Welch test for PCNA LI, TUNEL index, ratio of PCNA and TUNEL and MeDIP-PCR; Wilcoxon rank sum test for the grade of GSH immunostaining.

## Results

### Chemical analysis of arsenicals in the liver

Because metabolism of inorganic arsenic is a critical step for toxicity development<sup>13, 14</sup>, we measured As(V), As(III), MMA, DMA, and TMA in liver samples from male and female rats receiving 80 mg/kg/day of CCA. The results revealed that DMA was 5.8- or 3.1-fold higher than As(V) in male and female rats, respectively (Table 3). The level of DMA was almost same between male and female rats, while the levels of As(V) and MMA in female rats were about 2-fold higher than those in males. The levels of As(III) and MMA were lower than As(V) and TMA was not detected in

male and female rats.

### Measurement of cell proliferation and apoptosis

We randomly counted the number of PCNA- and TUNEL-positive hepatocytes in a hepatic lobule because there were no differences in interlobular distribution of the positive nuclei (centrilobular, midzonal, and periportal regions) (Fig. 1A and 1B). In the CCA 80 mg/kg/day group, the average of PCNA LI tended to be increased compared to the control group (control, 0.47%; 80 mg/kg/day, 2.28%;

**Table 3.** Arsenicals (mg/kg Tissue) in Liver Samples from Rats Treated with 80 mg/kg/day of Chromated Copper Arsenate

Arsenicals	Male	Female
As(V)	0.55 ± 0.09	1.08 ± 0.49
As(III)	0.07 ± 0.03	0.08 ± 0.04
MMA	0.15 ± 0.02	0.26 ± 0.25
DMA	3.17 ± 0.37	3.40 ± 0.27
TMA	ND	ND

The data are shown as arsenate (As[V]), arsenite (As[III]), and methylated forms, monomethylated-arsenic (MMA), dimethylated-arsenic (DMA), and trimethylated-arsenic (TMA).

ND: Not detected.

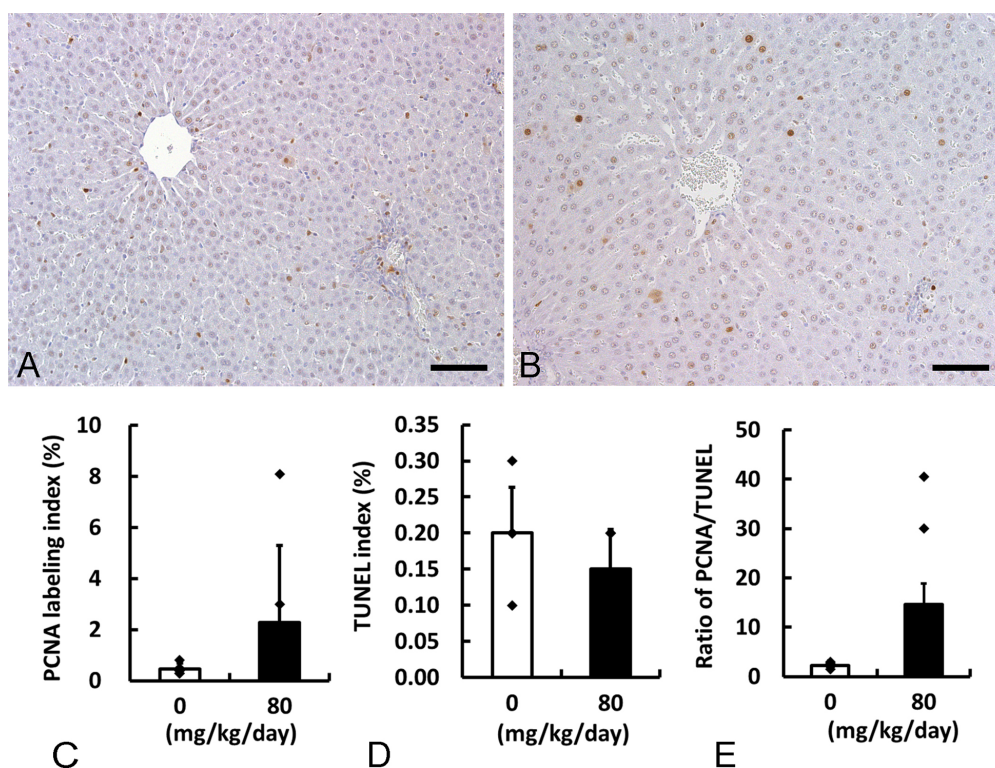


**Fig. 1.** Cell proliferation and apoptosis in the liver of female rats after 4-week wood preservative chromated copper arsenate exposure. Representative image of proliferating cell nuclear antigen (PCNA) in control (A) and 80 mg/kg/day treated female rats (B). Bar=50  $\mu$ m. Quantitative analysis in PCNA labeling index (C) and terminal deoxynucleotidyl transferase-mediated dUTP nick-end labeling (TUNEL) index (D). Calculation of ratio between PCNA labeling and TUNEL indices (E). N=6.

Fig. 1A–C), although no statistically significant difference was detected. High PCNA LIs were noted in three out of six females (Fig. 1C). The TUNEL index in the 80 mg/kg/day group tended to be decreased compared to that in the control group (control, 0.20%; 80 mg/kg/day, 0.15%; Fig. 1D). Thus, the ratio of PCNA and TUNEL was higher in the 80 mg/kg/day groups than that in the control group (control, 2.28; 80 mg/kg/day, 14.58; Fig. 1E). When the correlation between PCNA and TUNEL was determined, the correlation coefficient ( $r$ ) was 0.714 and 0.136 for the control and 80 mg/kg/day groups, respectively. The results indicated that the balance between cell proliferation and apoptosis was tilted in the direction of proliferation in the CCA-treated group.

#### Semi-quantitative analysis of GSH immunostaining

We visualized PSSG in the liver using immunohistochemistry with an anti-GSH antibody. In contrast to only a slight staining around the central vein in the control group, the positive region within the liver lobule was evidently expanded in the CCA-treated group (Fig. 2A and 2B), and the grade for GSH immunostaining was significantly higher in the CCA-treated group than in the control group (Table 4), suggesting a significant increase in PSSG in the liver when exposed to CCA.

#### Gene expression analysis by cDNA microarray and quantitative RT-PCR

In microarray analysis, genes that showed a change of more than 2-fold compared to those in the control group were selected as genes altered by CCA 80 mg/kg/day treatment. Among approximately 2,000 genes examined using microarray analysis, 56 and 8 genes were up- and down-regulated, respectively, in the CCA 80 mg/kg/day group as shown in Table 5. The genes were divided into categories, such as antioxidant, GST, HSP and ubiquitin-proteasome pathway, DNA repair, cell proliferation, negative regulator of cell proliferation, apoptosis, DNA methylation, cytochrome P450, glucose and lipid metabolism, transporter and genes related to hormones.

Genes involved in antioxidation (*Gclm*, *Blvra*, *Prdx2*,

*Car3*, *Rnh1*, *Prdx6*) were upregulated, while one metallothionein gene *Mtl* was downregulated in the microarray data. A significant decrease in *Mtl* was noted in the CCA 80 mg/kg/day group by confirmatory RT-PCR (Fig. 3). Consistent with these antioxidant-related changes, we detected increased expression of genes related to GST (*Gsta2*, *Gstm5*, *Gstl*, *Mgst1*) in the microarray data. Expression of two genes out of the four was confirmed by quantitative RT-PCR, and statistically significant increases in gene expression of *Gsta2* and *Mgst1* were observed in the CCA 40 and 80 mg/kg/day groups (Fig. 3). It was confirmed that *Gsta3* was upregulated in the same CCA treated groups by quantitative RT-PCR (Fig. 3), although it was not listed in the 2,000 genes of the microarray. Another mechanism to control oxidative stress damage in cells is exerted by an increase in HSP expression to renature damaged proteins and increase in the expression of genes involved in ubiquitination to degrade damaged proteins<sup>23</sup>. Upregulation of HSP and genes related to ubiquitin-proteasome pathway (*Ubb*, *Hspb3*, *Psmc4*, *Cryab*, *Tcp1*, *Psmc5*, *Dnajal1*) were detected by microarray. The DNA repair-related gene *Nudt1* was upregulated. *Nudt1*, also known as *Mth1*, is an 18 kD Nudix pyrophosphatase that hydrolyzes oxidized purine deoxyribonucleotides in the nucleotide pool, 8-oxo-dGTP, as well as the less frequently occurring 2-OH-dATP and 8-oxo-dATP<sup>24</sup>. Therefore, upregulation of *Nudt1*, and the increase

**Table 4.** Semi-quantitative Analysis of Glutathione Immunostaining

Grade	Dose level (mg/kg/day)	
	0	80
[N=]	[6]	[6]
+	3	0
++	3	1
+++	0	5
Statistical significance		**

[N=]: Number of animals examined.  
Significantly different from control: \*\* $p \leq 0.01$   
(Wilcoxon rank sum test).

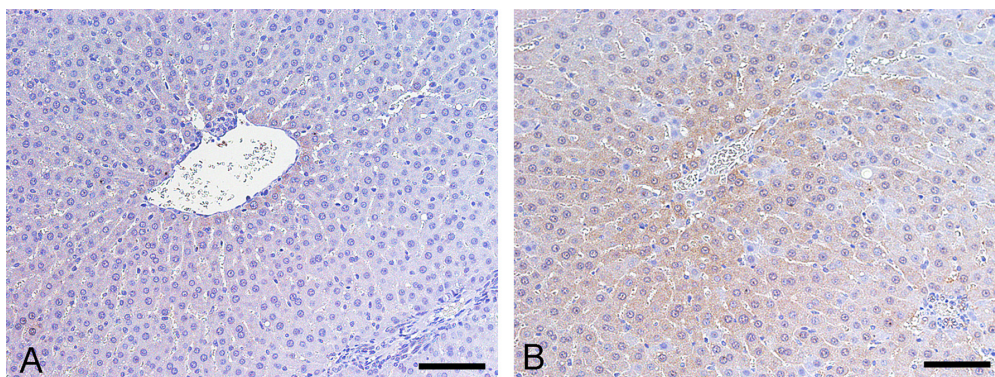


**Fig. 2.** Representative images of glutathione immunostaining in the liver of female rats after 4-week wood preservative chromated copper arsenate exposure. (A) A control female. (B) An 80 mg/kg/day treated female. Bar=50  $\mu$ m.

in 8-OHdG observed in our previous study<sup>12</sup>, suggested an increase in oxidative stress in the CCA-treated liver.

The many genes related to cell proliferation (*Pak1*, *Eif2s1*, *Ctcf*, *Camkk1*, *G3bp1*, *Stk39*, *Ptpn2*, *Plk1*, *Cdc25a*, *Wt1*) were positively regulated, while alteration in the negative regulation of cell proliferation (*Crlf3*, *Cdkn1b/p27*) was also observed to a lesser extent. Additionally, a cell proliferation-related gene, *Cdk1* was downregulated. A significant increase in *Cdkn1b/p27* was observed in the CCA 80 mg/kg/day group and confirmed by quantitative RT-PCR (Fig. 3). For apoptosis-related genes, two genes involved in the induction of apoptosis (*Tmsb10*, *Pawr*) were upregulated and a gene related to the inhibition of apoptosis (*Igf1*) was downregulated.

The DNA methylation-related gene, *Ctcf* was downregulated, and a significant decrease in *Ctcf* was noted in the CCA 80 mg/kg/day group by confirmatory RT-PCR (Fig. 3). Additional RT-PCR examination revealed that *Dnmt1* and *Dnmt3a* were downregulated in the CCA 40 and 80 mg/kg/day groups (Fig. 3).

The expression of various drug-metabolizing enzyme genes were also altered. The increased expression of six cytochrome P450 genes (*Cyp51*, *Cyp3a23/3a1*, *Cyp2e1*, *Cyp2f4*, *Cyp11b2*, *Cyp2c22*) and decreased expression of two cytochrome P450 genes (*Cyp4b1*, *Cyp3a9*) were detected. Three genes of glucose and lipid metabolism (*Dhcr7*, *Dpp4*, *Fabp5*) were increased, while one gene *Apoa4* was decreased. These changes in cytochrome P450 expression, and glucose and lipid metabolism could be related to diffuse hepatocellular hypertrophy with hyperglycemia and hypercholesterolemia observed in our previous study<sup>12</sup>. Five genes of transporter (*Slc29a1*, *Slc10a1*, *P2rx4*, *Slc17a7*, *P2rx1*) and three hormone-related genes (*Hsd11b1*, *Nr3c2*, *Pgrmc1*) were upregulated. Other miscellaneous genes, including im-

mune response were upregulated (*Olr59*, *Mgp*, *Ebf1*, *Dusp6*, *Vps33b*, *Avpr1a*, *Mmp2*) or downregulated (*C3*).

#### DNA methylation analysis in the promoter region of *Mt1* by quantitative MeDIP-PCR

Gene expression analysis revealed that *Mt1* mRNA was significantly downregulated in the CCA 80 mg/kg/day group. To examine how CCA mediates the expression of *Mt1*, methylation status in the promoter region of the *Mt1* was analyzed with the MeDIP-PCR method. We designed three primer and probe sets to cover the DNA sequence of one non-CGI (nCGI) and two CGI sites (CGIs 1 and 2) of the rat *Mt1* gene. Contrary to our expectations, the methylation status of all three sites examined in the CCA 80 mg/kg/day group were comparable or relatively lower than those in the control group, and the methylation status in both CCA 0 and 80 mg/kg/day groups was low (Fig. 4).

## Discussion

The liver is a potential target of toxic arsenic in humans, and arsenic exposure causes liver injuries, followed by the development of liver cancer<sup>15</sup>. Studies of human arsenic exposure and arsenic administration to experimental animal models have reported hepatocellular degeneration, hepatic inflammation and fibrosis, and cirrhosis in the liver<sup>25</sup>. We previously reported that 4-week repeated oral administration of 40 and 80 mg/kg/day of CCA induced diffuse hepatocellular hypertrophy in all female rats, but not in all male rats; among them, one male and one female rat treated with 80 mg/kg/day showed focal hepatocellular necrosis and bile duct hyperplasia with higher serum levels of aspartate aminotransferase and alanine aminotransferase<sup>12</sup>. In addition, female rats showed more pronounced

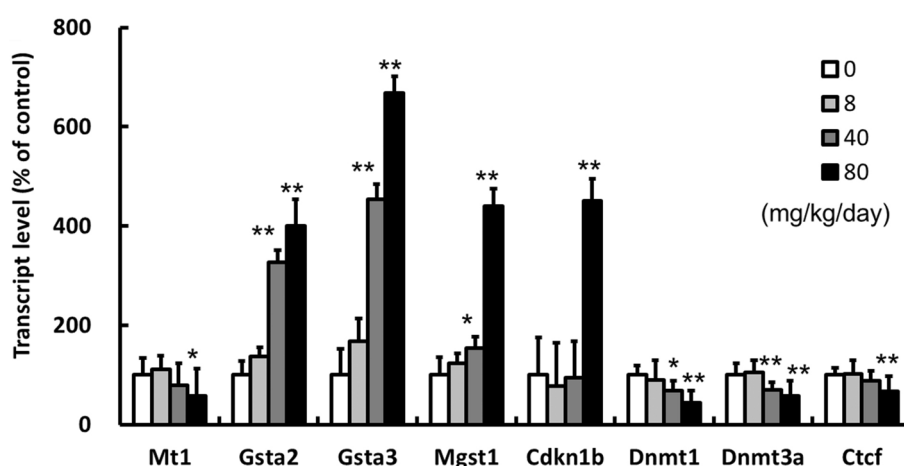


**Fig. 3.** Transcriptional levels of genes related to antioxidant, GST, cell proliferation, and DNA methylation in the liver of female rats after 4-week wood preservative chromated copper arsenate exposure at dose levels of 0, 8, 40, and 80 mg/kg/day. The data consists of metallothionein 1 (*Mt1*), glutathione S-transferase alpha 2 (*Gsta2*), glutathione S-transferase alpha 3 (*Gsta3*), microsomal glutathione S-transferase 1 (*Mgst1*), cyclin-dependent kinase inhibitor 1B (*Cdkn1b/p27*), DNA methyltransferase 1 (*Dnmt1*), DNA methyltransferase 3 alpha (*Dnmt3a*), and CCCTC-binding factor (*Ctcf*) and is presented as a percentage of the control levels. \* $p \leq 0.05$  or \*\* $p \leq 0.01$  versus control group by Dunnett's multiple comparison test.  $N = 10$ .

**Table 5.** Microarray Analysis of Gene Expression in the Liver from Female Rats Treated with 80 mg/kg/day of Chromated Copper Arsenate

Gene name	Gene symbol	Accession no.	Fold change
<b>Antioxidant</b>			
glutamate cysteine ligase, modifier subunit	<i>Gclm</i>	NM_017305	3.30
biliverdin reductase A	<i>Blvra</i>	NM_053850	2.94
peroxiredoxin 2	<i>Prdx2</i>	NM_017169	2.24
carbonic anhydrase 3	<i>Car3</i>	NM_019292	2.21
ribonuclease/angiogenin inhibitor 1	<i>Rnh1</i>	NM_139105	2.17
peroxiredoxin 6	<i>Prdx6</i>	NM_053576	2.00
metallothionein 1	<i>Mt1</i>	NM_138826	0.47
<b>Glutathione-S-transferase</b>			
glutathione S-transferase alpha 2	<i>Gsta2</i>	NM_017013	2.95
glutathione S-transferase, mu 5	<i>Gstm5</i>	NM_172038	2.10
glutathione S-transferase theta 1	<i>Gstt1</i>	NM_053293	2.10
microsomal glutathione S-transferase 1	<i>Mgst1</i>	NM_134349	2.03
<b>Heat shock proteins and ubiquitin-proteasome pathway</b>			
ubiquitin B	<i>Ubb</i>	NM_138895	3.48
heat shock protein family B (small) member 3	<i>Hspb3</i>	NM_031750	2.70
proteasome 26S subunit, non-ATPase 4	<i>Psm4</i>	NM_031331	2.64
crystallin, alpha B	<i>Cryab</i>	NM_012935	2.48
t-complex 1	<i>Tcp1</i>	NM_012670	2.29
proteasome 26S subunit, ATPase 5	<i>Psmc5</i>	NM_031149	2.15
DnaJ heat shock protein family (Hsp40) member A1	<i>Dnaj1</i>	NM_022934	2.00
<b>DNA repair</b>			
nudix hydrolase 1	<i>Nudt1 (Mth1)</i>	NM_057120	2.52
<b>Cell proliferation</b>			
p21 (RAC1) activated kinase 1	<i>Pak1</i>	NM_017198	3.36
eukaryotic translation initiation factor 2 subunit 1 alpha	<i>Eif2s1</i>	NM_019356	2.76
connective tissue growth factor	<i>Ctgf</i>	NM_022266	2.72
calcium/calmodulin-dependent protein kinase kinase 1	<i>Camkk1</i>	NM_031662	2.64
G3BP stress granule assembly factor 1	<i>G3bp1</i>	AB032425	2.63
serine threonine kinase 39	<i>Stk39</i>	NM_019362	2.38
protein tyrosine phosphatase, non-receptor type 2	<i>Ptpn2</i>	NM_053990	2.20
polo-like kinase 1	<i>Plk1</i>	NM_017100	2.20
cell division cycle 25A	<i>Cdc25a</i>	NM_133571	2.15
Wilms tumor 1	<i>Wt1</i>	NM_031534	2.08
cyclin-dependent kinase 1	<i>Cdk1</i>	NM_019296	0.41
<b>Negative regulation of cell proliferation</b>			
cytokine receptor-like factor 3	<i>Crlf3</i>	AF072835	2.52
cyclin-dependent kinase inhibitor 1B	<i>Cdkn1b (p27)</i>	NM_031762	2.15
<b>Apoptosis</b>			
thymosin, beta 10	<i>Tmsb10</i>	NM_021261	2.86
pro-apoptotic WT1 regulator	<i>Pawr</i>	NM_033485	2.09
insulin-like growth factor 1	<i>Igf1</i>	M15481	0.46
<b>DNA methylation</b>			
CCCTC-binding factor	<i>Ctcf</i>	NM_031824	0.45
<b>Cytochrome P450</b>			
cytochrome P450, family 51	<i>Cyp51</i>	NM_012941	4.65
cytochrome P450, family 3, subfamily a, polypeptide 23/ polypeptide 1	<i>Cyp3a23/3a1</i>	NM_013105	4.54
cytochrome P450, family 2, subfamily e, polypeptide 1	<i>Cyp2e1</i>	NM_031543	3.50
cytochrome P450, family 2, subfamily f, polypeptide 4	<i>Cyp2f4</i>	NM_019303	2.10
cytochrome P450, family 11, subfamily b, polypeptide 2	<i>Cyp11b2</i>	NM_012538	2.06
cytochrome P450, family 2, subfamily c, polypeptide 22	<i>Cyp2c22</i>	NM_138512	2.04
cytochrome P450, family 4, subfamily b, polypeptide 1	<i>Cyp4b1</i>	NM_016999	0.45
cytochrome P450, family 3, subfamily a, polypeptide 9	<i>Cyp3a9</i>	NM_147206	0.41

**Table 5.** Continued

Gene name	Gene symbol	Accession no.	Fold change
Glucose and lipid metabolism			
7-dehydrocholesterol reductase	<i>Dhcr7</i>	NM_022389	2.15
dipeptidylpeptidase 4	<i>Dpp4</i>	NM_012789	2.08
fatty acid binding protein 5, epidermal	<i>Fabp5</i>	NM_145878	2.00
apolipoprotein A4	<i>Apoa4</i>	NM_012737	0.39
Transporter			
solute carrier family 29 member 1	<i>Slc29a1</i>	NM_031684	3.42
solute carrier family 10 member 1	<i>Slc10a1</i>	NM_017047	3.36
purinergic receptor P2X 4	<i>P2rx4</i>	NM_031594	2.54
solute carrier family 17 member 7	<i>Slc17a7</i>	NM_053859	2.18
purinergic receptor P2X 1	<i>P2rx1</i>	NM_012997	2.00
Genes related to hormone			
hydroxysteroid 11-beta dehydrogenase 1	<i>Hsd11b1</i>	NM_017080	3.36
nuclear receptor subfamily 3, group C, member 2	<i>Nr3c2</i>	NM_013131	2.31
progesterone receptor membrane component 1	<i>Pgrmc1</i>	NM_021766	2.09
Others			
olfactory receptor 59	<i>Olr59</i>	NM_173293	2.88
matrix Gla protein	<i>Mgp</i>	NM_012862	2.76
early B-cell factor 1	<i>Ebfl</i>	NM_053820	2.45
dual specificity phosphatase 6	<i>Dusp6</i>	NM_053883	2.08
VPS33B, late endosome and lysosome associated	<i>Vps33b</i>	NM_022286	2.00
arginine vasopressin receptor 1A	<i>Avpr1a</i>	NM_053019	2.00
matrix metalloproteinase 2	<i>Mmp2</i>	NM_031054	2.00
complement C3	<i>C3</i>	NM_016994	0.38

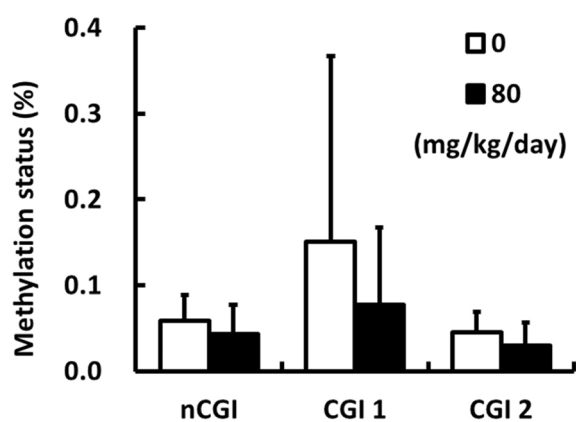


**Fig. 4.** Methylation status in the promoter region of *Mtl*. The data are shown in the non-CGI site (nCGI), first CGI (CGI 1), and third CGI closest to the transcription start site (CGI 2). The female rats were orally treated with 0 or 80 mg/kg/day of chromated copper arsenate for 4 weeks. N=6.

blood biochemical changes indicative of hepatotoxicity than males. The sex difference in CCA-mediated hepatotoxicity had not been elucidated, and in this study, we measured the concentrations of several arsenical species in the liver tissues from male and female rats exposed to 80 mg/kg/day for four weeks. Inorganic arsenic is enzymatically methylated to mono- and di-methylated species (MMA and DMA) in human and experimental animals and detected at high levels in the liver<sup>13, 14</sup>. We found that DMA was the major

metabolite in the liver tissue in this study, although we did not confirm the ratio of dimethylarsinic acid (DMA[V]) and dimethylarsinous acid (DMA[III]), which is highly reactive and responsible for arsenic toxicity<sup>14</sup>. As the concentrations of As(V) and MMA in female rats were higher than in males, the differences in arsenic distribution may be the cause of the differences in liver response. Although it is not clear why As(V) and MMA concentrations were higher in female rats than in males, it might be due to sex differences in arsenic metabolism, such as higher methylation capacity, which metabolizes As(III) to MMA, and lower purine nucleoside phosphorylase (PNP) activity, which reduces As(V) to As(III), in female rats than in males<sup>26</sup>.

As(III) is sequentially methylated to form methylarsonate (MMA[V]) and DMA(V) by arsenic methyltransferase (AS3MT or Cyt19) using S-adenosylmethionine (SAM) as a methyl group donor<sup>13, 14</sup>. SAM is also required for most other cellular methylation reactions, including DNA methylation<sup>27</sup>. Chronic exposure of rat liver epithelial cells to inorganic arsenic induces SAM depletion, causing a global loss of DNA methylation during malignant transformation<sup>28</sup>. Chronic exposure to inorganic arsenic produces hepatic DNA hypomethylation<sup>29, 30</sup>. Global hypomethylation of DNA is one of the most important nongenotoxic mechanisms of carcinogenesis that acts by facilitating aberrant gene expression and can be a causative factor in hepatocarcinogenesis<sup>31</sup>. On the other hand, arsenic-mediated hypermethylation in the transcriptional regulatory regions of genes has been proposed to silence tumor suppressor genes<sup>32</sup>. Consequently, arsenic exposure might be associat-

ed with both hypo- and hyper-methylation at various genetic loci. In this study, a significant decrease in *Mt1* mRNA was observed in the CCA 80 mg/kg/day group. *Mt1* is an important molecule in the cellular defense system and its cysteine residues have been reported to scavenge reactive oxygen species (ROS)<sup>33</sup>. Thus, the downregulation of *Mt1* mRNA was considered to play an important role in the hepatotoxicity induced by CCA. Although *Mt1* cannot bind arsenic, it acts as a protective factor by scavenging ROS. Ghoshal et al. reported that induced inhibition of the *Mt1* gene in rat hepatoma cells was due to hypermethylation of the gene promoter<sup>34</sup>. In this study, however, we did not demonstrate a significant change in DNA methylation in the promoter regions of *Mt1* in the liver of female rats exposed to 80 mg/kg/day of CCA. Methyl groups are added to cytosine residues by DNA methyltransferase (Dnmt) and the methyl group donor is SAM. There is evidence that arsenic alters Dnmt activity and subsequently the DNA methylation patterns in cells<sup>32</sup>. For the DNA methylation-related genes examined in this study, *Ctcf*, *Dnmt1*, and *Dnmt3a* were downregulated by CCA exposure. *Ctcf* is a highly conserved zinc finger protein, best known as a transcription factor. The protein is also known to play a role in DNA methylation; it can function as a transcriptional activator, repressor or insulator, blocking the communication between enhancers and promoters<sup>35, 36</sup>. Interestingly, arsenic has been shown to inhibit *Ctcf* binding to DNA<sup>37, 38</sup>. Rea et al. reported that arsenic-induced inhibition in *Ctcf* at the promoter region of *Dnmts* resulted in the repression of gene expression of *Dnmts*<sup>36</sup>. Thus, CCA-induced inhibition of *Ctcf* might be associated with the repression of gene expression of *Dnmt1* and *Dnmt3a*. This downregulated *Dnmt1* and *Dnmt3a* would be related to relatively low methylation statuses in the promoter region of the *Mt1*. However, we demonstrated that CCA silenced *Mt1* gene transcription in a DNA methylation-independent manner in the present study. With respect to chromium, one of the components of the CCA, Cr(VI) inhibits *Mt1* transcription by modifying the transcriptional potential of the co-activator p300 in mouse embryo fibroblast cells<sup>39</sup>. Further study is needed to elucidate the mechanism of inhibition of *Mt1* transcription by CCA or the combined effects of arsenic and chromium.

The balance between cell proliferation and cell death is important for the maintenance of organs. Arsenic decreases hepatocyte volume in the liver after administration via drinking water to rats for 8 weeks<sup>40</sup>, and *in vitro* exposure of hepatocytes to arsenic induced apoptosis and decreased cell proliferation<sup>41, 42</sup>. These changes were accompanied by decreased expression of antioxidant enzymes, including superoxide dismutase and catalase<sup>41, 42</sup>. The development of arsenic toxicity likely resulted from the action of several mechanisms of toxicity, including the alteration of protein function via direct binding to sulfhydryl groups as well as the generation of oxidative stress<sup>25</sup>. Oxidative stress, in turn, can damage cellular macromolecules, such as proteins, lipids, and DNA<sup>25</sup>. Chromium also induces apoptosis in the liver after administration via drinking water to rats for 10

weeks<sup>43</sup>. In contrast, we demonstrated that CCA caused increased PCNA LI and decreased TUNEL index, suggesting that the balance was tilted in the direction of proliferation in association with the altered gene expression in cell proliferation, negative regulator of cell proliferation, and apoptosis in microarray analysis. The discrepancy between our study and previous studies on cell proliferation and apoptosis is uncertain, but it might be dependent on the study design and combined effects of CCA components. In this study, we observed altered gene expression related to antioxidants and GST, which were confirmed by quantitative RT-PCR. Therefore, our data suggested that CCA-mediated oxidative stress might be involved in hepatotoxicity by impairing the balance between apoptosis and cell proliferation in female rats treated with CCA, and the results might be related to hepatocarcinogenesis as reported in arsenic exposure<sup>15</sup>.

In our previous study, CCA increased 8-OHdG levels in female rat livers, possibly due to arsenic and chromium-mediated oxidative stress<sup>12</sup>. The microarray results showed increased expression of genes involved in antioxidant functions (*Gclm*, *Blvra*, *Prdx2*, *Car3*, *Rnh1*, *Prdx6*), which have a potential to reduce oxidative stress. GSH also has strong antioxidant properties, but an increase in PSSG was immunohistochemically observed in hepatocytes at 80 mg/kg/day in this experiment, suggesting that CCA decreased the reduced form of GSH<sup>20</sup>. The result is consistent with the finding in arsenic-exposed rats; following oral intake of arsenic, the GSH concentration was significantly decreased in the liver of male Wistar rats<sup>25</sup>. Additionally, GSH plays a central role in metabolism of reducing pentavalent arsenic to trivalent arsenic and is utilized in the conjugation process to remove metabolites from the body<sup>44, 45</sup>. In association with these reactions, glutamate cysteine ligase modifier subunit (*Gclm*), the primary rate-limiting enzyme for glutathione synthesis, was increased in microarray analysis, suggesting an enhancement of the GSH synthesis system due to GSH depletion by CCA<sup>46</sup>. The increased expression of  $\gamma$ -glutamyl transpeptidase, as shown in the blood biochemistry in our previous study<sup>12</sup>, might be associated with a pathway that degrades extracellular GSH and re-uptakes cysteine to re-synthesize GSH<sup>46</sup>. Disturbances in GSH homeostasis have been associated with liver diseases induced by drugs, alcohol, diet, and environmental pollutants<sup>16, 46</sup>. Therefore, GSH depletion might be a major cause of CCA hepatotoxicity observed in female rats. The redox steady state of GSH and the oxidized form of GSH (GSSG) (i.e., the GSH/GSSG ratio) is crucial for cellular signaling processes in cell proliferation and apoptosis<sup>20</sup>, that could cause the imbalance between proliferation and apoptosis in the liver when exposed to CCA. Consistent with these antioxidant-related changes, we detected increased expression of genes related to GST (*Gsta2*, *Gsta3*, *Gstm5*, *Gstl*, *Mgst1*) by microarray and quantitative RT-PCR analyses. The expression of GST-mu, GST-pi, GST-alpha, and GST-theta were all increased by *in utero* arsenic exposure in the livers of newborn mice<sup>47</sup>. GSTs are a large group of enzymes, and some of them are able to catalyze the conjugation of GSH with arsenic<sup>30, 48, 49</sup>.

Increased GST expression and activity, particularly GST-pi, play important roles in arsenic adaptation through increased cellular efflux of arsenic-GSH conjugates<sup>48, 49</sup>. GST expression and its activity in humans are also associated with altered arsenic metabolism<sup>50, 51</sup>, and GST polymorphisms may be a susceptibility factor for human arsenic toxicity<sup>51</sup>. Taken together, these data indicate that disruption of GST gene expression are events consistent with arsenic associated carcinogenicity and toxicity.

Our current and previous studies<sup>12</sup> suggest that dimethylated arsenic-mediated decrease in GSH and altered gene expression of antioxidants, including inhibition of Mtl transcription, GST, and DNA methylation might cause hepatotoxicity in the liver of female rats treated with CCA. The limitations of this study include that we measured metabolites of arsenic but did not confirm the deposition of metabolites of Cr(VI) and Cu in liver tissues when exposed to CCA. Administration of arsenic in drinking water can also alter the concentrations of Zn, Mg, Na, Ca, and Cu in the liver of rats<sup>40</sup>. Further studies on the combination of As, Cr, and Cu-mediated cell responses are required to better understand the mechanism of hepatotoxicity of CCA.

**Disclosure of Potential Conflicts of Interest:** The authors declared that they have no conflicts of interest.

**Acknowledgment:** We thank Ms. Mutsumi Kumagai, Takako Kazami, Yukie Sakano, Chizuko Tomiyama, Kayoko Iijima, Junko Fukumori, and Mr. Satoshi Akema for tissue preparation. We especially thank Dr. Nobuaki Nakashima, Dr. Yukiko Kashimoto, and the deceased Dr. Maki Kuwahara. This work was supported by a grant in aid of research on risk assessment of wood preservatives from the Ministry of Health, Labour and Welfare, Japan.

## References

- Morais S, Fonseca H, Oliveira SMR, Oliveira H, Gupta VK, Sharma B, and de Lourdes Pereira M. Environmental and health hazards of chromated copper arsenate-treated wood: a review. *Int J Environ Res Public Health*. **18**: 5518. 2021. [Medline] [CrossRef]
- Katz SA, and Salem H. Chemistry and toxicology of building timbers pressure-treated with chromated copper arsenate: a review. *J Appl Toxicol*. **25**: 1–7. 2005. [Medline] [CrossRef]
- US EPA Chromated Arsenicals (CCA). Last updated on February 4, 2022. website: <https://www.epa.gov/ingredients-used-pesticide-products/chromated-arsenicals-cca1.2.3>.
- Englot C. Treated wood-managing the risk. In: Environmental Impacts of Treated Wood. TG Townsend, and H Solo-Gabriele (eds). CRC Press, Boca Raton. (Chapter 17). [6]. Jambeck J. The Disposal. 2006.
- Shibata T, Solo-Gabriele HM, Fleming LE, Cai Y, and Townsend TG. A mass balance approach for evaluating leachable arsenic and chromium from an in-service CCA-treated wood structure. *Sci Total Environ*. **372**: 624–635. 2007. [Medline] [CrossRef]
- Deramos King CM, Dozier CS, Campbell JL, Curry ED, and Godri Pollitt KJ. Long-term leaching of arsenic from pressure-treated playground structures in the northeastern United States. *Sci Total Environ*. **656**: 834–842. 2019. [Medline] [CrossRef]
- Townsend T, Tolaymat T, Solo-Gabriele H, Dubey B, Stook K, and Wadanambi L. Leaching of CCA-treated wood: implications for waste disposal. *J Hazard Mater*. **114**: 75–91. 2004. [Medline] [CrossRef]
- Mercer TG, and Frostick LE. Evaluating the potential for environmental pollution from chromated copper arsenate (CCA)-treated wood waste: a new mass balance approach. *J Hazard Mater*. **276**: 10–18. 2014. [Medline] [CrossRef]
- Ohgami N, Yamanoshita O, Thang ND, Yajima I, Nakano C, Wenting W, Ohnuma S, and Kato M. Carcinogenic risk of chromium, copper and arsenic in CCA-treated wood. *Environ Pollut*. **206**: 456–460. 2015. [Medline] [CrossRef]
- Mason RW, and Edwards IR. Acute toxicity of combinations of sodium dichromate, sodium arsenate and copper sulphate in the rat. *Comp Biochem Physiol C Comp Pharmacol Toxicol*. **93**: 121–125. 1989. [Medline] [CrossRef]
- Mason RW, Edwards IR, and Fisher LC. Teratogenicity of combinations of sodium dichromate, sodium arsenate and copper sulphate in the rat. *Comp Biochem Physiol C Comp Pharmacol Toxicol*. **93**: 407–411. 1989. [Medline] [CrossRef]
- Takahashi N, Yoshida T, Kojima S, Yamaguchi S, Ohtsuka R, Takeda M, Kosaka T, and Harada T. Pathological and clinical pathological changes induced by four-week, repeated-dose, oral administration of the wood preservative chromated copper arsenate in Wistar rats. *Toxicol Pathol*. **46**: 312–323. 2018. [Medline] [CrossRef]
- Thomas DJ, Styblo M, and Lin S. The cellular metabolism and systemic toxicity of arsenic. *Toxicol Appl Pharmacol*. **176**: 127–144. 2001. [Medline] [CrossRef]
- Watanabe T, and Hirano S. Metabolism of arsenic and its toxicological relevance. *Arch Toxicol*. **87**: 969–979. 2013. [Medline] [CrossRef]
- Tokar EJ, Benbrahim-Tallaa L, Ward JM, Lunn R, Sams RL 2nd, and Waalkes MP. Cancer in experimental animals exposed to arsenic and arsenic compounds. *Crit Rev Toxicol*. **40**: 912–927. 2010. [Medline] [CrossRef]
- Xu M, Rui D, Yan Y, Xu S, Niu Q, Feng G, Wang Y, Li S, and Jing M. Oxidative damage induced by arsenic in mice or rats: a systematic review and meta-analysis. *Biol Trace Elem Res*. **176**: 154–175. 2017. [Medline] [CrossRef]
- American Wood Preservers Association. American Wood Preservers Association Standards. American Wood Preservers Association, Selma. 2005.
- Japanese Association for Laboratory Animal Science (JALAS). Guidelines for animal experimentation. *Exp Anim*. **36**: 285–288. 1987.
- Takahashi N, Yoshida T, Ohnuma A, Horiuchi H, Ishitsuka K, Kashimoto Y, Kuwahara M, Nakashima N, and Harada T. The enhancing effect of the antioxidant N-acetylcysteine on urinary bladder injury induced by dimethylarsinic acid. *Toxicol Pathol*. **39**: 1107–1114. 2011. [Medline] [CrossRef]
- Giustarini D, Colombo G, Garavaglia ML, Astori E, Portinaro NM, Reggiani F, Badalamenti S, Aloisi AM, Santucci A, Rossi R, Milzani A, and Dalle-Donne I. Assessment of glutathione/glutathione disulphide ratio and S-glutathio-

- nylated proteins in human blood, solid tissues, and cultured cells. *Free Radic Biol Med.* **112**: 360–375. 2017. [[Medline](#)] [[CrossRef](#)]
21. Harada T, Yamaguchi S, Ohtsuka R, Takeda M, Fujisawa H, Yoshida T, Enomoto A, Chiba Y, Fukumori J, Kojima S, Tomiyama N, Saka M, Ozaki M, and Maita K. Mechanisms of promotion and progression of preneoplastic lesions in hepatocarcinogenesis by DDT in F344 rats. *Toxicol Pathol.* **31**: 87–98. 2003. [[Medline](#)] [[CrossRef](#)]
  22. Yang YH, Dudoit S, Luu P, Lin DM, Peng V, Ngai J, and Speed TP. Normalization for cDNA microarray data: a robust composite method addressing single and multiple slide systematic variation. *Nucleic Acids Res.* **30**: e15. 2002. [[Medline](#)] [[CrossRef](#)]
  23. Leonard SS, Harris GK, and Shi X. Metal-induced oxidative stress and signal transduction. *Free Radic Biol Med.* **37**: 1921–1942. 2004. [[Medline](#)] [[CrossRef](#)]
  24. Maki H, and Sekiguchi M. MutT protein specifically hydrolyses a potent mutagenic substrate for DNA synthesis. *Nature.* **355**: 273–275. 1992. [[Medline](#)] [[CrossRef](#)]
  25. Jomova K, Jenisova Z, Feszterova M, Baros S, Liska J, Hudecova D, Rhodes CJ, and Valko M. Arsenic: toxicity, oxidative stress and human disease. *J Appl Toxicol.* **31**: 95–107. 2011. [[Medline](#)]
  26. Muhetaer M, Yang M, Xia R, Lai Y, and Wu J. Gender difference in arsenic biotransformation is an important metabolic basis for arsenic toxicity. *BMC Pharmacol Toxicol.* **23**: 15. 2022. [[Medline](#)] [[CrossRef](#)]
  27. Baylin SB, Herman JG, Graff JR, Vertino PM, and Issa JP. Alterations in DNA methylation: a fundamental aspect of neoplasia. *Adv Cancer Res.* **72**: 141–196. 1998. [[Medline](#)] [[CrossRef](#)]
  28. Zhao CQ, Young MR, Diwan BA, Coogan TP, and Waalkes MP. Association of arsenic-induced malignant transformation with DNA hypomethylation and aberrant gene expression. *Proc Natl Acad Sci USA.* **94**: 10907–10912. 1997. [[Medline](#)] [[CrossRef](#)]
  29. Chen H, Li S, Liu J, Diwan BA, Barrett JC, and Waalkes MP. Chronic inorganic arsenic exposure induces hepatic global and individual gene hypomethylation: implications for arsenic hepatocarcinogenesis. *Carcinogenesis.* **25**: 1779–1786. 2004. [[Medline](#)] [[CrossRef](#)]
  30. Xie Y, Trouba KJ, Liu J, Waalkes MP, and Germolec DR. Biokinetics and subchronic toxic effects of oral arsenite, arsenate, monomethylarsonic acid, and dimethylarsinic acid in v-Ha-ras transgenic (Tg.AC) mice. *Environ Health Perspect.* **112**: 1255–1263. 2004. [[Medline](#)]
  31. Watson RE, and Goodman JI. Effects of phenobarbital on DNA methylation in GC-rich regions of hepatic DNA from mice that exhibit different levels of susceptibility to liver tumorigenesis. *Toxicol Sci.* **68**: 51–58. 2002. [[Medline](#)] [[CrossRef](#)]
  32. Reichard JF, and Puga A. Effects of arsenic exposure on DNA methylation and epigenetic gene regulation. *Epigenomics.* **2**: 87–104. 2010. [[Medline](#)] [[CrossRef](#)]
  33. Thornalley PJ, and Vasák M. Possible role for metallothionein in protection against radiation-induced oxidative stress. Kinetics and mechanism of its reaction with superoxide and hydroxyl radicals. *Biochim Biophys Acta.* **827**: 36–44. 1985. [[Medline](#)] [[CrossRef](#)]
  34. Ghoshal K, Majumder S, Li Z, Dong X, and Jacob ST. Suppression of metallothionein gene expression in a rat hepatoma because of promoter-specific DNA methylation. *J Biol Chem.* **275**: 539–547. 2000. [[Medline](#)] [[CrossRef](#)]
  35. Chang J, Zhang B, Heath H, Galjart N, Wang X, and Milbrandt J. Nicotinamide adenine dinucleotide (NAD)-regulated DNA methylation alters CCCTC-binding factor (CTCF)/cohesin binding and transcription at the BDNF locus. *Proc Natl Acad Sci USA.* **107**: 21836–21841. 2010. [[Medline](#)] [[CrossRef](#)]
  36. Rea M, Eckstein M, Eleazer R, Smith C, and Fondufe-Mittendorf YN. Genome-wide DNA methylation reprogramming in response to inorganic arsenic links inhibition of CTCF binding, DNMT expression and cellular transformation. *Sci Rep.* **7**: 41474. 2017. [[Medline](#)] [[CrossRef](#)]
  37. Miao Z, Wu L, Lu M, Meng X, Gao B, Qiao X, Zhang W, and Xue D. Analysis of the transcriptional regulation of cancer-related genes by aberrant DNA methylation of the cis-regulation sites in the promoter region during hepatocyte carcinogenesis caused by arsenic. *Oncotarget.* **6**: 21493–21506. 2015. [[Medline](#)] [[CrossRef](#)]
  38. Rojas D, Rager JE, Smeester L, Bailey KA, Drobná Z, Rubio-Andrade M, Stýblo M, Garcia-Vargas G, and Fry RC. Prenatal arsenic exposure and the epigenome: identifying sites of 5-methylcytosine alterations that predict functional changes in gene expression in newborn cord blood and subsequent birth outcomes. *Toxicol Sci.* **143**: 97–106. 2015. [[Medline](#)] [[CrossRef](#)]
  39. Kimura T, Okumura F, Onodera A, Nakanishi T, Itoh N, and Isobe M. Chromium (VI) inhibits mouse metallothionein-I gene transcription by modifying the transcription potential of the co-activator p300. *J Toxicol Sci.* **36**: 173–180. 2011. [[Medline](#)] [[CrossRef](#)]
  40. Souza ACF, Marchesi SC, de Almeida Lima GD, and Machado-Neves M. Effects of Arsenic Compounds on Microminerals Content and Antioxidant Enzyme Activities in Rat Liver. *Biol Trace Elem Res.* **183**: 305–313. 2018. [[Medline](#)] [[CrossRef](#)]
  41. Bera AK, Rana T, Bhattacharya D, Das S, Pan D, and Das SK. Sodium arsenite-induced alteration in hepatocyte function of rat with special emphasis on superoxide dismutase expression pathway and its prevention by mushroom lectin. *Basic Clin Pharmacol Toxicol.* **109**: 240–244. 2011. [[Medline](#)] [[CrossRef](#)]
  42. Rana T, Bera AK, Das S, Bhattacharya D, Pan D, Bandyopadhyay S, De S, and Das SK. Mushroom lectin protects arsenic induced apoptosis in hepatocytes of rodents. *Hum Exp Toxicol.* **30**: 307–317. 2011. [[Medline](#)] [[CrossRef](#)]
  43. Rafael AI, Almeida A, Santos P, Parreira I, Madeira VM, Alves R, Cabrita AM, and Alpoim MC. A role for transforming growth factor-beta apoptotic signaling pathway in liver injury induced by ingestion of water contaminated with high levels of Cr(VI). *Toxicol Appl Pharmacol.* **224**: 163–173. 2007. [[Medline](#)] [[CrossRef](#)]
  44. Stýblo M, Venkatratnam A, Fry RC, and Thomas DJ. Origins, fate, and actions of methylated trivalent metabolites of inorganic arsenic: progress and prospects. *Arch Toxicol.* **95**: 1547–1572. 2021. [[Medline](#)] [[CrossRef](#)]
  45. Wadgaonkar P, and Chen F. Connections between endoplasmic reticulum stress-associated unfolded protein response, mitochondria, and autophagy in arsenic-induced carcinogenesis. *Semin Cancer Biol.* **76**: 258–266. 2021. [[Medline](#)] [[CrossRef](#)]
  46. Chen Y, Dong H, Thompson DC, Shertzer HG, Nebert DW,

- and Vasiliou V. Glutathione defense mechanism in liver injury: insights from animal models. *Food Chem Toxicol.* **60**: 38–44. 2013. [[Medline](#)] [[CrossRef](#)]
47. Xie Y, Liu J, Benbrahim-Tallaa L, Ward JM, Logsdon D, Diwan BA, and Waalkes MP. Aberrant DNA methylation and gene expression in livers of newborn mice transplacentally exposed to a hepatocarcinogenic dose of inorganic arsenic. *Toxicology.* **236**: 7–15. 2007. [[Medline](#)] [[CrossRef](#)]
48. Liu J, Chen H, Miller DS, Saavedra JE, Keefer LK, Johnson DR, Klaassen CD, and Waalkes MP. Overexpression of glutathione S-transferase II and multidrug resistance transport proteins is associated with acquired tolerance to inorganic arsenic. *Mol Pharmacol.* **60**: 302–309. 2001. [[Medline](#)] [[CrossRef](#)]
49. Leslie EM, Haimeur A, and Waalkes MP. Arsenic transport by the human multidrug resistance protein 1 (MRP1/ABCC1). Evidence that a tri-glutathione conjugate is required. *J Biol Chem.* **279**: 32700–32708. 2004. [[Medline](#)] [[CrossRef](#)]
50. Chiou HY, Hsueh YM, Hsieh LL, Hsu LI, Hsu YH, Hsieh FI, Wei ML, Chen HC, Yang HT, Leu LC, Chu TH, Chen-Wu C, Yang MH, and Chen CJ. Arsenic methylation capacity, body retention, and null genotypes of glutathione S-transferase M1 and T1 among current arsenic-exposed residents in Taiwan. *Mutat Res.* **386**: 197–207. 1997. [[Medline](#)] [[CrossRef](#)]
51. Marnell LL, Garcia-Vargas GG, Chowdhury UK, Zakharyan RA, Walsh B, Avram MD, Kopplin MJ, Cebrián ME, Silbergeld EK, and Aposhian HV. Polymorphisms in the human monomethylarsonic acid (MMA V) reductase/hGSTO1 gene and changes in urinary arsenic profiles. *Chem Res Toxicol.* **16**: 1507–1513. 2003. [[Medline](#)] [[CrossRef](#)]